A Unified Roche-Model Light Curve Solution for the W UMa Binary AC Bootis

Kevin B. Alton
UnderOak Observatory, 70 Summit Avenue, Cedar Knolls, NJ 07927; kbalton@optonline.net

Received June 8, 2009; revised October 8, 2009; accepted October 8, 2009

Abstract Over forty years of photoelectric light curves published by five different investigators and CCD data more recently (2006) collected in *V*- and *R*-bands were analyzed using a Roche-type geometry as implemented by the Wilson-Devinney code. This has not only resulted in a revised ephemeris and orbital period for AC Boo, but has lead to a unified light curve solution. Based upon moments of minima residual analysis, AC Boo has experienced a continual increase in orbital period for the past forty-eight years or longer, thereby suggesting an ongoing exchange of mass. Fourier analysis also revealed possible periodicity in O–C residuals which is heavily influenced by a putative sinusoidal-like wave most apparent over the past twenty years. The weight of evidence, nonetheless, points to a W-subtype W UMa system that does not necessarily vary as the result of an unseen companion (third light) but rather by spot formation on either stellar component. A series of spotted solutions, based upon a nearly symmetrical light curve collected in 1962, has provided a theoretical fit of all published photoelectric data that largely accounts for the observed peak asymmetry, unequal successive maxima, and varying depths of minima.

1. Introduction

The variability of AC Bootis was first discovered in 1955 (Geyer) and since then studied by a number investigators, including Binnendijk (1965), Mauder (1964), Mancuso *et al.* (1977, 1978), Schieven *et al.* (1983), Robb (1985), Linnell *et al.* (1990), and Hrivnak (1993). This binary system completes mutual eclipses in a little more than eight hours (0.35245 day). Typical of the W UMa class of overcontact binaries, many light curves exhibit peak asymmetry visible as unequal heights of successive maxima, which has been referred to as the O'Connell effect. AC Boo belongs to the W-type subclass of W UMa binaries, since the less massive but hotter star is occulted by the more massive but cooler component during primary minimum (Tsesevich 1956, 1959). The spectral type of the primary component is listed as F8Vn (Bilir *et al.* 2005). Our view of this system is nearly edge-on (orbital inclination ~84°), so the eclipses are total/annular.

Historically, model fits to photometric data on individual W UMa variables like AC Boo have varied significantly across investigations with respect to orbital

inclination (i), Roche potential (Ω), T_{eff}, and mass ratio (q). Since fundamental changes to these physical elements likely transpire over millennia, rather than measured in human lifetimes, the expectation is that these parameters should have remained fairly constant over just fifty-plus years of recorded photometric data. If a reference set of values can be established for i, Ω, T_1, T_2, and q, epochal variations in light curve morphology could potentially be modeled by the addition of putative spot(s) or by the presence of additional orbital mass within the gravitational influence of the binary system (also known as "third light"). Although the inspiration for this exercise with AC Boo pre-dates a recent public challenge (Ruciński *et al.* 2009) to combine light curve data extant for individual systems, the rationale is self-evident. Given the wide range of reported values for fundamental physical properties of binary star systems, there have been improbably small uncertainties established for each parameter. Public access to software applications like PHOEBE (PHysics Of Eclipsing BinariEs; Prša and Zwitter 2005), PERIOD04 (Lenz and Breger 2005), MINIMA (Nelson 2005b), and WDWINT (Nelson 2005c), has expanded the repertoire of user-friendly light curve modeling tools to amateur astronomers. For those so inclined, this greatly facilitates the retrospective analysis of published data which is the main focus of this paper. Having said that, with the advances made in affordable optics and CCD cameras, the modern amateur astronomer can also generate new research-quality light curves for variable star systems that had in the past only been within the domain of the professional community. In this regard, AC Boo is well suited for study, since this relatively bright variable (Vmag ~10) is easily within the detection limits of a consumer-grade CCD camera coupled with a telescope of modest aperture. During the late spring months, this system passes near zenith for mid-latitude observers in the Northern Hemisphere.

2. Observations and data reduction

2.1. Astrometry

Images of AC Boo were matched against the standard star fields provided in MPO CANOPUS (Minor Planet Observer 1996–2008) as described previously for SW Lac (Alton and Terrell 2006).

2.2. Photometry

CCD photometric observations of AC Boo began on 29 April 2006 with the intent of generating light curves which could be used to: 1) potentially refine the orbital period, 2) calculate an updated ephemeris, and 3) further investigate the light curve asymmetry regularly observed for this system. Equipment included a 0.2-meter catadioptric (f/6.4) reflector with an SBIG ST-402ME CCD camera mounted at primary focus. V- or R-band imaging was carried out during separate sessions through Schüler photometric filters (1.25-inch) based upon the Johnson-Cousins Bessell prescription. A more detailed description and performance characteristics of this photometric system has been described elsewhere by Alton

(2006) and Alton and Terrell (2006). Each unbinned exposure was captured over a fifteen-second period with thermoelectric cooling regulated to maintain the CCD chip 20°C below the initial ambient temperature. A typical session lasted from two to four hours, with images taken every sixty seconds. PC clock time was updated via the Internet Time Server immediately prior to each session. Image acquisition (raw lights, darks, and flats) was performed using SBIG CCDSOFT 5 while calibration and registration were accomplished with AIP4WIN (Berry and Burnell 2000). Photometric reduction with MPO CANOPUS used at least three non-varying comparison stars. Instrumental readings were not reduced to standard magnitudes before generating light curves to calculate ephemerides and orbital period. Phased differential magnitude photometric data in all passbands published by Binnendijk (1965), Mauder (1964), Mancuso *et al.* (1977, 1978), Robb (1985), and Schieven *et al.* (1983) were converted to flux ($F = 10^{-0.4*\Delta m}$) and then normalized.

2.3. Light curve analyses

Light curve modeling was performed using PHOEBE (Prša and Zwitter 2005) and WDWINT (Nelson 2005c), both of which employ the Wilson-Devinney (W-D) code (Wilson and Devinney 1971; Wilson 1979). PHOEBE is a well-designed execution of the W-D code which provides a convenient user interface. Each model fit incorporated individual observations and was not binned to normal points. SIGMA was assigned according to the standard deviation measured from the average difference in instrumental magnitude (C_{avg}) for each comparison star. For the *V* and *R* passbands, variability was typically ±0.03 magnitude. Three-dimensional representations showing the location of putative starspot(s) were rendered by BINARY MAKER 3.0 (Bradstreet and Steelman 2002).

3. Results and discussion

3.1. Astrometry

The position determined for AC Boo (Table 1) based upon the reference coordinates in the *MPO Star Catalog* (Minor Planet Observer 2008) agreed within 0.441 arcsec of right ascension or declination reported on the SIMBAD website (ICRS 2000 coordinates).

Table 1. Positions and magnitudes of AC Boo and comparison stars.

Star Identification	*R.A.* *h m s*	*Dec.* ° ′ ″	V_T *mag*	B_T *mag*
AC Boo	14 56 28.33	+46 21 44.1	10.294	10.849
TYC3474-00966-1	14 56 26.31	+46 26 51.0	9.434	9.817
TYC3474-00714-1	14 56 19.60	+46 19 08.8	12.394	12.943
TYC3474-00835-1	14 56 07.82	+46 21 26.6	11.242	11.841

3.2. Ensemble photometry

Every attempt was made to ensure that comparison stars were themselves not variable, at least over the observation time span. This was verified prior to accepting data from each session. On any night, no less than three stars from the *Tycho2 Catalogue* (Høg *et al.* 2000) were used for differential measurements. The airmass for all observations over the entire campaign ranged from 1.048 to 1.792. Plotting the difference in magnitude over time for AC Boo against the averaged magnitude for all comparisons (C_{avg}) yielded a narrow range of values with no obvious trend (Figure 1). Collectively, C_{avg} for the comparison stars did not exhibit a pattern that would otherwise suggest variability beyond experimental error (< 0.03 magnitude) in both passbands.

3.3. Folded light curve and ephemerides

Photometric readings in *V* (942) and *R* (890) passbands produced seven times of minima (ToM) which were captured during eight viewing sessions between 29 April 2006 and 17 July 2006. The Fourier analysis routine (Harris *et al.* 1989) in MPO CANOPUS provided a period solution. A ToM for the latest primary epoch was estimated by CANOPUS using the Hertzsprung method as detailed by Henden and Kaitchuck (1990). As such the linear ephemeris equation (1) was initially determined to be:

$$\text{Min I (hel.)} = 2453932.5819 + 0.352457(69)\text{E} \quad (1)$$

This orbital period based upon a limited dataset compares favorably with values reported by Binnendijk (1965), Mancuso *et al.* (1977, 1978), Schieven *et al.* (1983), Robb (1985), Linnell *et al.* (1990), and Demircan *et al.* (2003). Periodograms produced using PERANSO (Vanmunster 2005) by applying periodic orthogonals (Schwarzenberg-Czerny 1996) to fit observations and analysis-of-variance to evaluate fit quality also confirmed the period determination. ToM values for all epochs were then separately estimated by MINIMA (Nelson 2005b) using the simple mean from a suite of six different methods including parabolic fit, tracing paper, bisecting chords, Kwee and van Woerden (1956), Fourier fit, and sliding integrations (Ghedini 1981). These seven new minima along with additional published CCD observations (*IBVS* and *Var. Star Bull.* as provided in the reference list) were entered into a MICROSOFT EXCEL spreadsheet adapted from the "Eclipsing Binary O–C" files developed by Nelson (2005a). Using the following reference epoch from Kreiner (2004):

$$\text{Min I (hel.)} = 2452500.3020\ (9) + 0.3524485\ (1)\ \text{E} \quad (2)$$

new ephemerides were established for AC Boo (Table 1). Due to the complex curvilinear nature of the O–C residuals observed for at least forty-eight years (Figure 2), two separate regression analyses were performed. A revised ephemeris equation (3) based upon a linear least squares fit (Figure 3) of near term $(O–C)_1$ data from 16 Feb 2006 to 07 May 2009 was calculated:

$$\text{Min I (hel.)} = 2452499.9500\,(9) + 0.3524484\,(2)\,E \quad (3)$$

As a result of the parabolic O–C vs time relationship, updated linear elements for AC Boo may only be valid for a short time after 2009. Expanding the analysis to include O–C data starting from 18 Jan 1961 revealed a parabolic relationship (Figure 2) between daily residuals $(O–C)_1$ and time (cycle number) that could be fit by a quadratic expression (4):

$$O–C = a + bE + cE^2 \quad (4)$$

where:

$a = –0.33910 \quad \pm 0.0008$
$b = –4.6351 \times 10^{-6} \quad \pm 0.1090 \times 10^{-6}$
$c = 2.3003 \times 10^{-10} \quad \pm 0.03789 \times 10^{-10}$

This solution which is defined by an upwards parabola ($c > 0$) suggests that the period is increasing linearly with time and leads to the following quadratic ephemeris (5):

$$\text{Min I (hel.)} = 2452499.9629\,(8) + 0.3524439\,(1)\,E + 2.300\,(38) \times 10^{-10}\,E^2 \quad (5)$$

Since 1961 the orbital period rate of increase can be defined by the equation (6) below:

$$dP/dt = 2 \times (2.300 \times 10^{-10})\,(1/0.3524439)\,(86400)\,(365.25) = 0.0412\ \text{sec/yr} \quad (6)$$

Commonly observed in W UMa binary systems, orbital period increases may be associated with material transfer from the secondary to the more massive primary component. Recalculated quadratic residuals, $(O–C)_Q$, are shown in the bottom panel of Figure 2. There is a visual suggestion of a sinusoidal-like wave particularly over the past twenty years that was further examined using PERANSO Lomb-Scargle periodogram analysis (Vanmunster 2005) and discrete Fourier analysis as implemented in PERIOD04 (Lenz and Breger 2005). Both mathematical approaches are particularly effective at least squares fitting of sine waves with unevenly sampled data. The highest peak (c/d) in each power spectrum corresponded to periods ranging between 7,225 ± 1,091 days (PERANSO) and 7,553 ± 658 days (PERIOD04); peak amplitude was estimated to be ~0.009 day. Two other statistical algorithms within PERANSO yielded similar values with equal or higher error estimates. These included date compensated discrete Fourier Transform DCDFT (Ferraz-Mello 1981) and CLEANEST (Foster 1995). The sinusoidal-like fit (Figure 4) of quadratic O–C residuals between 18 Jan 1961 and 07 May 2009 is strongly influenced by Time of Minimum (ToM) values collected over the past twenty years. Given the scatter in residuals prior to cycle –14,000, it will probably require at least twenty years of additional data to confirm this putative periodicity with statistical certainty. Whether this behavior is real, associated with a third body, or some other cyclic phenomena such as the "Applegate mechanism" (Applegate 1992), remains to be determined. Applegate

proposed that a late-type short-period binary system consisting of at least one star with a convective envelope would exhibit a magnetic activity cycle analogous to the eleven-year solar sunspot cycle. Variable tidal effects (physical distortion) would be observed as changes in the orbital period of the binary system which may be regular but not exactly periodic. The presence of a third body has been proposed by Hrivnak (1993) and Linnell (1991), based on radial velocity data collected around cycle –13,000 (est. 1989). Collectively, however, despite the putative presence of a sinusoidal-like feature over the past twenty years, there still is not enough evidence from the analysis of O–C vs time plots to argue unequivocally for persistent periodicity, a prerequisite for third light effects. In addition, it should be noted that no improvement in any light curve model fit using W-D code (Wilson and Devinney 1971; Wilson 1979) could be obtained with a non-zero value for third light (l_3); differential corrections including l_3 as a variable did not lead to a statistically significant non-zero solution.

With regard to the 2006 photometric readings, folded light curves incorporating all observations (Figure 5) in *V*- and *R*-passbands show that both minima are separated by 0.5 phase, an observation consistent with a circular orbit. Although the light curve in *R* has a gap at Max I due to poor weather, asymmetry in maximum light (Max I > Max II) is clearly seen in *V*-band. Both passbands exhibit unequal depths at minima (Min I < Min II). With the exception of the 1962 light curves (*B* and *V*) reported by Binnendijk (1965) which have near equal maximum light and matching minima, all others produced since then have had asymmetric maxima along with near equal minima (Mancuso *et al.* 1977; Schieven *et al.* 1983), or unequal minima (Binnendijk 1965; Mauder 1964; Robb 1985; and the present paper).

A plausible explanation for this variability attributed to the O'Connell effect might involve the changing presence of starspot(s) on one or more binary components and is explored in more detail below. A recent publication by Wilsey and Beaky (2009) provides an excellent overview of the O'Connell effect in eclipsing binary systems. Therein a number of theoretical models which could explain the diagnostic out-of-eclipse asymmetry at maximum light are discussed. The most thoroughly published approach to model this effect has been to invoke the presence of starspot(s). Analogous to differential rotation on the Sun, localized magnetic disturbances on W UMa binaries can block convective motion towards the surface and result in cool starspots which may survive for a protracted period of time (Berdyugina 2005). Alternatively, hot spots akin to solar flares may also appear but can be expected to evolve in a more transient manner. Both phenomena disturb luminous homogeneity and can produce asymmetric features on a light curve. The W-D code has been designed to accommodate the introduction of idealized circular starspots to improve the model fit, a software feature not implemented for any of the alternative theories which account for light curve asymmetry. Not unexpectedly, this limitation which fails to address other sources of light curve variability has perhaps led to overuse of starspot modeling. As mentioned earlier, a parabolic relationship (Figure 2) between daily residuals and time is often

attributed to conservative mass transfer. This sets the stage for an alternative theory in which a superluminous spot is produced by the impact of a streaming flow of gaseous matter through L1, the inner Lagrangian point. If the hotspot is offset from the central axis (not at 90° co-latitude, 0° longitude in W-D parlance), then a difference in luminosity can be observed during Max I or Max II. Taking a sneak look ahead, this scenario is suggested by the spotted W-D model fit of the 2006 light curve (Figure 15). Another less conventional explanation for the O'Connell effect involves a variation on the gas-stream impact theory in which the two components sweep through and capture matter in cloud of circumstellar material, thereby converting kinetic energy into a thermal glow on each leading hemisphere (Liu and Yang 2003). It remains to be seen whether this explanation will be supported by spectroscopic evidence, since an increased incidence of emission lines is expected along with a difference in spectra captured at Min I and Min II. Still another theory invokes the presence of an asymmetrically dense circumbinary cloud of gas and/or dust which directly attenuates light at different orbital phases (Lehmann and Mkrtichian 2004). Finally Zhou and Leung (1990) proposed that the asymmetric deflection of an incoming stream of matter due to Coriolis forces can account for unequal light curve maxima in an over-contact binary. To date, no one of these alternative theories has accumulated sufficient experimental evidence to completely supplant the presence of starspot(s) as the most viable explanation for the O'Connell effect.

3.4. Roche modeling and light curve analyses

Model fits to photometric data from individual W UMa variables like AC Boo vary significantly in the literature with respect to orbital inclination (i), Roche potential (Ω), T_{eff}, and mass ratio (q). Since these basic physical elements likely change over millennia, their individual reported uncertainties are unrealistically small. Being nearly symmetrical, the 1962 light curves from Binnendijk (1965) offer an opportunity to create a reference set of values for i, Ω, T_1, T_2, and q. Thereafter, epochal variations in light curve morphology could potentially be explained by additional orbital mass within the gravitational influence of the binary system (also known as "third light") or the presence of putative spot(s).

For overcontact binary systems of the W UMa type, W-D light curve solutions generally employ "mode 3" (a documented feature of the W-D code) with synchronous rotation and circular orbits. In this case, however, the "overcontact binary but not in thermal contact" option in PHOEBE yielded the best model fits. Since AC Boo has a convective envelope ($T_{eff} < 7500$ K), values for bolometric albedo (0.5) and gravity darkening exponents (0.32) were based on theoretical considerations described by Ruciński (1969) and Lucy (1967), respectively. Logarithmic limb darkening coefficients for both stars were interpolated within PHOEBE according to van Hamme (1993) with any change in temperature. AC Boo conforms to the W-subtype where the less massive but hotter star is eclipsed at primary minimum. Although the secondary and less-massive star has the higher

surface temperature, it nonetheless contributes less to the overall luminosity of this binary system due to its smaller size. Therefore, T_{eff} for the primary (T_1) was set equal to 6252 K, based on tabulated values (de Jager and Nieuwenhuijzen 1987) for an F8 main sequence dwarf star. Initial attempts to obtain a light curve fit involved adjustment of parameters for the mean effective temperature of the secondary (T_2), orbital inclination (i), mass ratio (q), bandpass-specific luminosity of the primary (L_1), and common envelope surface potential ($\Omega_1 = \Omega_2$). Once an approximate fit was obtained, differential corrections (DC) were applied simultaneously to photometric data in all filters. To alleviate strong correlations, the method of multiple subsets (Wilson and Biermann 1976) was used only when necessary to reach convergence.

3.4.1. Binnendijk 1962 light curves (*B* and *V*)

Although a spectroscopic mass ratio ($q = 0.41$) for AC Boo was determined by Hrivnak (1993), this value ultimately led to unrealistically complex fits when all light curves were considered. Fortunately, AC Boo exhibits total/annular eclipses, a pre-condition to obtaining a robust value for q by photometric means (Wilson 1994; Terrell and Wilson 2005). A new search for q was initiated by allowing this physical element to vary freely also with i, Ω, and T_2 during DC iterations. Simultaneously in both passbands, an excellent fit quickly converged at $q \sim 0.31$, so this parameter was investigated further under more controlled conditions. Mass ratio (q) was fixed over a range of 0.21 to 0.5 and the free model parameters (i, Ω, and T_2) allowed to converge. The response curve generated by plotting χ^2 as a function of the putative mass ratio showed a minimum between 0.30 and 0.32 (Figure 6). This value was further refined ($q = 0.306$) and thereafter used as the de facto mass ratio for modeling AC Boo. It should be noted that a very similar estimate for q had been previously reported by Mancuso *et al.* (1978) and Schieven *et al.* (1983). A comparison of light curves (Figure 7) from 0.28 to 0.41q reveals the sensitivity to mass ratio in achieving good model prediction during each eclipse. All that remained for this idealized light curve was to determine i, Ω, and T_2 by DC with fixed values for q and T_1. Final physical and geometrical elements from modeling the 1962 light curves for AC Boo are summarized in Table 2; synthetic light curves are illustrated in Figure 8.

3.4.2. Binnendijk 1963 light curves (*B* and *V*)

Not unexpectedly, the exact light curve solution for the 1962 data discussed above did not provide a best fit for AC Boo light curves produced before and thereafter. While trying to explain perturbations in radial velocity data, Hrivnak (1993) points to the possibility of a third body in the AC Boo system. In an earlier study reported by Linnell (1991), light curve data (which were not available for further analysis) required the introduction of 8% third light to obtain an accurate Roche model fit. Contrary to these assumptions, O–C residuals calculated from time-of-minima data which stretch back over forty-eight years do not exhibit the strict sinusoidal periodicity that one would expect from an orbiting third body

(Budding and Demircan 2007). Therefore, a strategy to build a Roche model was based on the premise that asymmetric maxima and/or unequal minima observed for AC Boo arise from starspot(s) on either component. BINARYMAKER 3 enabled visualization of spot placement so that combinations of A_S, Θ, ϕ, and r_S could be tested prior to final optimization with PHOEBE and WDWINT. Concerns regarding the use of starspots to minimize residuals during light curve synthesis have been well documented (Berdyugina 2005). Consequently, every effort was made to minimize the number of spots used to best fit each light curve. In some cases, due to the significant variability associated with each epoch two spots were required; the 1963 photometric readings from AC Boo were no exception in this regard. Results from modeling these light curves are summarized in Table 2 and illustrated in Figure 9. As can also be seen in subsequent light curve fits from four other epochs, a cool spot on the more massive star (Figure 15) which is exposed during primary eclipse serves to deepen Min I. In a similar, but opposing fashion, a hot spot located on the smaller companion body slightly brightened Min II during transit in the 1963 dataset.

3.4.3. Mauder 1961 light curves (*B* and *V*)

Light curves from Mauder (1964) were only available in graphical form, so photometric data (Δ mag) in *B*- and *V*-passbands were extracted using Dexter (Demleitner *et al.* 2001), a JAVA applet which allows the user to digitize a plot by creating an x-y coordinate system and then positioning a marker on each datum point. This utility is available on the NASA Astrophysics Data System website (http://adswww.harvard.edu/index.html) and can be directly invoked with GIF scanned articles. Physical and geometrical elements garnered from modeling these 1961 light curves for AC Boo are summarized in Table 2. Starspot locations (co-latitude and longitude) which improved the Roche model fit for these 1961 light curves from Mauder (1964) were very similar to those employed for the 1963 data acquired by Binnendijk (1965). With some exceptions discussed later, there was a tendency for maximum light after the secondary minimum to exhibit greater variability with transient excursions suggestive of flare activity (Figure 10).

3.4.4. Mancuso 1972 and 1973 light curves (*V*)

The results from modeling these photoelectrically derived light curves for AC Boo are summarized in Table 2 and plotted in Figure 11. As with previous light curves covering consecutive years (1961–1963), considerable differences were observed between 1972 and 1973. Most notably in 1973, maximum light appeared in the first quadrature, a feature shared only with the 1984 and 2006 light curves. In both Mancuso light curves the model supported placement of a subluminous spot on the more massive star (longitude = 180°) which served to deepen the primary minimum. Mancuso *et al.* (1978) reported for the first time geometric and physical elements for AC Boo estimated from a Roche-based model (Wilson and Devinney 1971). Given the assumptions and model limitations at that time, direct comparisons reveal values for *i* (85.47°), T_1 (5830–6017 K),

T_2 (6100 K), and q (0.28) that are reasonably close to those calculated herein (Table 2) using PHOEBE.

3.4.5. Schieven 1982 light curves (*U*, *B*, and *V*)

Arguably, upon first inspection (Figure 12), a case can be made that the light curves produced with *B* and *V* filters are equivalent from a standpoint of symmetry, maximum light, and depth of minima when compared to those generated in 1962 (Figure 8) by Binnendijk (1965). It should be pointed out that each plotted value represents the mean of four determinations, so that unlike in 1962, some of the variability has been smoothed out in the 1982 light curves. Successive minima appear nearly equal in depth across all passbands. However, without a hot starspot (Figure 15) positioned on the secondary star, a less than optimal fit to the Roche model was obtained in *B*- and *U*-passbands. This was particularly evident in the first quadrature following primary minimum. Schieven *et al.* (1983) only provided a partial list of physical elements determined from light curve synthesis. Notably, values for q (0.28–0.31) and i (82.6°–84.0°) are very consistent with findings reported herein (Table 2).

3.4.6. Robb 1984 light curves (*U*, *B*, and *V*)

As with Mauder (1964), AC Boo light curves produced by Robb (1985) were only available in a figure from a scanned copy of their publication. Photoelectric data (Δ mag) in *U*-, *B*-, and *V*-passbands were extracted on-line as described earlier using Dexter (Demleitner *et al.* 2001) and then converted to flux. The results from modeling these data are summarized in Table 2 and shown in Figure 13. Due to significant variability and frequent gaps in the data, an acceptable model fit for these light curves proved to be a challenge. Nonetheless, a reasonable fit was found by positioning a cool spot on the primary constituent (Figure 15).

3.4.7. Light curves (*V* and *R*) from 2006 study

Physical and geometric elements used and estimated in modeling these CCD observations are summarized in Table 2. Unequal minima, very apparent at visible wavelengths (Figure 14), were closer in depth as compared to those measured in *R*-passband. Due to uncooperative weather, a gap around maximum light still remained in the *R*-filtered dataset after the seasonal campaign on this star system was terminated. As mentioned earlier, maximum light which appeared in first quadrature was a feature common with the 1973 and 1984 light curves. In this case a hot spot positioned in the neck region (Figure 15) was effective in improving the model fit to the observed data near first quadrature.

4. Conclusions

Recent *V*- and *R*-filtered CCD-based observations have led to the construction of light curves which were used to: 1) revise the orbital period for AC Boo, 2) calculate updated ephemerides and, 3) further investigate the peak asymmetries

regularly observed for this system. A parabolic relationship between O–C residuals and cycle number has been derived which suggests continual period increases over nearly five decades. Fourier analysis of the associated quadratic residuals provided a hint, but not compelling evidence for strict sinusoidal periodicity occurring approximately every twenty-one years. Despite reports to the contrary, and until which time sufficient moments-of-minima data are collected from AC Boo, it would be premature to corroborate the gravitational influence of another body on this binary system. Using PHOEBE, analysis of photometric data covering the past forty-eight years and published by several investigators has produced a uniform solution of all light curves using Roche-based modeling. Epochal variability such as peak asymmetry, unequal successive maxima, and dissimilar minima was addressed by incorporating starspot(s) on one or both binary constituents. This has provided synthetic fits of light curve data that largely account for the observed differences.

5. Acknowledgements

The insightful comments from an anonymous referee, and the helpfulness and thorough work of the *JAAVSO* editorial and production staff are much appreciated and greatly improved the overall quality of this manuscript. The NASA Astrophysics Data System hosted by the Computation Facility at the Harvard-Smithsonian Center for Astrophysics is gratefully acknowledged. This investigation also made use of the SIMBAD database, operated at Centre de Données Astronomiques de Strasbourg (CDS), Strasbourg, France. Finally, special thanks is due to Dr. Andrej Prša for his personal assistance in using PHOEBE.

References

Agerer, F., and Hübscher, J. 1996, *Inf. Bull. Var. Stars*, No. 4382.
Agerer, F., and Hübscher, J. 1997, *Inf. Bull. Var. Stars*, No. 4472.
Agerer, F., and Hübscher, J. 1998, *Inf. Bull. Var. Stars*, No. 4606.
Agerer, F., and Hübscher, J. 2002, *Inf. Bull. Var. Stars*, No. 5296.
Agerer, F., and Hübscher, J. 2003, *Inf. Bull. Var. Stars*, No. 5484.
Aksu, O., *et al.* 2005, *Inf. Bull. Var. Stars*, No. 5588.
Alton, K. 2006, *Open Eur. J. Var. Stars*, **39**, 1.
Alton, K. B., and Terrell, D. 2006, *J. Amer. Assoc. Var. Star Obs.*, **34**, 188.
Applegate, J. H. 1992, *Astrophys. J.*, **385**, 621.
Bakis, V., Bakis, H., Erdem, A., Çiçek, C., Demircan, O., and Budding, E. 2003, *Inf. Bull. Var. Stars*, No. 5464.
Bakis, V., Dogru, S. S., Bakis, H., Dogru, D., Erdem, A., Çiçek, C., and Demircan, O. 2005, *Inf. Bull. Var. Stars*, No. 5662.
Berdyugina, S. V. 2005, *Living Rev. Sol. Phys.*, **2**, 8.
Berry, R., and Burnell, J. 2000–2006, "Astronomical Image Processing Software,"

version 2.1.10, provided with *The Handbook of Astronomical Image Processing*, Willmann-Bell, Richmond.
Bilir, S., Karataş, Y., Demircan, O., and Eker, Z. 2005, *Mon. Not. Roy. Astron. Soc.*, **357**, 2, 497.
Binnendijk, L. 1965, *Astron. J.*, **70**, 201.
Bradstreet, D. H., and Steelman, D. P. 2002, *Bull. Amer. Astron. Soc.*, **34**, 1224.
Budding, E., and Demircan, O. 2007, *Introduction to Astronomical Photometry*, Cambridge Univ. Press, Cambridge, UK.
de Jager, C., and Nieuwenhuijzen, H. 1987, *Astron. Astrophys.*, **177**, 217.
Demircan, O., *et al.* 2003, *Inf. Bull. Var. Stars*, No. 5364.
Demleitner, M., Accomazzi, A., Eichhorn, G., Grant, C. S., Kurtz, M. J., and Murray, S. S. 2001, in *Astronomical Data Analysis Software and Systems X*, eds. F. R. Harnden, Jr., F. A. Primini, and H. E. Payne, Astron. Soc. Pacific Conf. Ser., 238, Astron. Soc. Pacific, San Francisco, 321.
Diethelm, R. 2005, *Inf. Bull. Var. Stars*, No. 5653.
Diethelm, R. 2006, *Inf. Bull. Var. Stars*, No. 5713.
Diethelm, R. 2009, *Inf. Bull. Var. Stars*, No. 5894.
Dogru, S. S., Dogru, D., Erdem, A., Çiçek, C., and Demircan, O. 2006, *Inf. Bull. Var. Stars*, No. 5707.
Dvorak, S.W. 2006, *Inf. Bull. Var. Stars*, No. 5677.
Dvorak, S.W. 2008, *Inf. Bull. Var. Stars*, No. 5814.
Ferraz-Mello, S. 1981, *Astron. J.*, **86**, 619.
Foster, G. 1995, *Astron. J.*, **109**, 1889.
Geyer, E. 1955, *Bamberg Kleine Veröff. der Remeis-Sternwarte*, **9**, 4.
Ghedini, S. 1981, *Mem. Soc. Astron. Italia*, **52**, 633.
Harris, A. W., *et al.* 1989, *Icarus*, **77**, 171.
Henden, A. A., and Kaitchuck, R. H. 1990, *Astronomical Photometry: A Text and Handbook for the Advanced Amateur and Professional Astronomer*, Willmann-Bell, Richmond.
Høg, E., *et al.*, 2000, *The Tycho-2 Catalogue of the 2.5 Million Brightest Stars, Astron. Astrophys.*, **355**, L27.
Hrivnak, B. J. 1993, in *New frontiers in binary star research: a colloquium sponsored by the U.S. National Science Foundation and the Korean Science and Engineering Foundation, Seoul and Taejon, Korea, November 5-13, 1990,* eds. K-C. Leung and I-S. Nha, Astron. Soc. Pacific Conf. Ser. 38, Astron. Soc. Pacific, San Francisco, 269.
Hübscher, J. 2005, *Inf. Bull. Var. Stars*, No. 5643.
Hübscher, J. 2007, *Inf. Bull. Var. Stars*, No. 5802.
Hübscher, J., Paschke, A., and Walter, F. 2005, *Inf. Bull. Var. Stars*, No. 5657.
Hübscher, J., Paschke, A., and Walter, F. 2006, *Inf. Bull. Var. Stars*, No. 5731.
Hübscher, J., Steinbach, H-M., and Walter, F. 2008, *Inf. Bull. Var. Stars*, No. 5830.
Hübscher, J., Steinbach, H-M., and Walter, F. 2009, *Inf. Bull. Var. Stars*, No. 5874.
Hübscher, J., Steinbach, H-M., and Walter, F. 2009, *Inf. Bull. Var. Stars*, No. 5889.
Hübscher, J., and Walter, F. 2007, *Inf. Bull. Var. Stars*, No. 5761.

Kiliçoglu, T., *et al.* 2007, *Inf. Bull. Var. Stars*, No. 5801.
Kim, C-H., Lee, C-U., Yoon, Y-N., Park, S-S., Kim, D-H., Cha, S-M., and Won, J-H. 2006, *Inf. Bull. Var. Stars*, No. 5694.
Kreiner, J. M. 2004, *Acta Astron.*, **54**, 207.
Kwee, K. K., and van Woerden, H. 1956, *Bull. Astron. Inst. Netherlands*, **12**, 327.
Lehmann, H., and Mkrtichian, D. E. 2004, *Astron. Astrophys.*, **413**, 293.
Lenz, P., and Breger, M. 2005, PERIOD04 v1.1.1 software, *Commun. Asteroseismology*, **146**, 53.
Linnell, A. P. 1991, in *The Sun and Cool Stars. Activity, Magnetism, Dynamos*, eds. I. Tuominen, D. Moss, and G. Rudiger, Proc. IAU Colloq. 130, Helsinki, July 17–20, 1990, Springer-Verlag, Berlin, 376.
Linnell, A. P., Hrivnak, B., and Olson, E. C. 1990, *Bull. Amer. Astron. Soc.*, **22**, 1291.
Liu, Q., and Yang, Y. 2003, *Chinese J. Astron. Astrophys.*, **3**, 142.
Lucy, L. B. 1967, *Z. Astrophys.*, **65**, 89.
Maciejewski, G., and Karska, A. 2004, *Inf. Bull. Var. Stars*, No. 5494.
Mancuso, S., Milano, L., and Russo, G. 1977, *Astron. Astrophys. Suppl.*, **29**, 57.
Mancuso, S., Milano, L., and Russo, G. 1978, *Astron. Astrophys., Suppl. Ser.*, **63**, 193.
Mauder, H. 1964, *Z. Astrophys.*, **60**, 222.
Minor Planet Observer 1996–2008, MPO CANOPUS (version 9.5.0.3), and *PhotoRed Installation Guide and Reference Manual*, BDW Publishing, Colorado Springs (http://www.minorplanetobserver.com).
Nagai, K. 2003, *Var. Star Bull.*, **40**, 1.
Nagai, K. 2004, *Var. Star Bull.*, **42**, 2.
Nagai, K. 2005, *Var. Star Bull.*, **43**, 1.
Nagai, K. 2006, *Var. Star Bull.*, **44**, 2.
Nelson, R. 2001, *Inf. Bull. Var. Stars*, No. 5040.
Nelson, R. 2004, *Inf. Bull. Var. Stars*, No. 5493.
Nelson, R. 2005a, "Eclipsing Binary O–C," (http://www.aavso.org/observing/programs/eclipser/omc/).
Nelson, R. 2005b, MINIMA (version 24d) astronomy software, http://members.shaw.ca/bob.nelson/software1.htm
Nelson, R. 2005c, WDWINT (version 5.4e) astronomy software, http://members.shaw.ca/bob.nelson/software1.htm
Nelson, R. 2008, *Inf. Bull. Var. Stars*, No. 5820.
Parimucha, S., Dubovsky, P., Baludansky, D., Pribulla, T., Hambálek, L., Vanko, M., and Ogloza, W. 2009, *Inf. Bull. Var. Stars*, No. 5898.
Pejcha, O. 2005, *Inf. Bull. Var. Stars*, No. 5645.
Prša, A., and Zwitter, T. 2005, *Astrophys. J.*, **628**, 1, 426.
Robb, R. M. 1985, *Inf. Bull. Var. Stars*, No. 2764.
Ruciński, S. M. 1969, *Acta Astron.*, **19**, 245.
Ruciński, S. M., *et al.* 2009, "Commission 42, Triennial Report 2006–2009," to appear in *Trans. IAU, Reports on Astronomy*, **27A**, ed. K. A. van der Hucht, Cambridge, Univ. Press, Cambridge.

Safár, J., and Zejda, M. 2002, *Inf. Bull. Var. Stars*, No. 5263.
Schieven, G., Morton, J. C., McLean, B. J., and Hughes, V. A. 1983, *Astron. Astrophys., Suppl. Ser.*, **52**, 463.
Schwarzenberg-Czerny, A. 1996, *Astrophys. J., Lett.*, **460**, L107.
Senavci, H. V., *et al.* 2007, *Inf. Bull. Var. Stars*, No. 5754.
Terrell, D., and Wilson, R. E. 2005, *Astrophys. Space Sci.*, **296**, 221.
Tsesevich, V. P. 1956, *Astron. Tsirk.*, **171**, 20.
Tsesevich, V. P. 1959, *Astron. Tsirk.*, **173**, 14.
van Hamme, W. 1993, *Astron. J.*, **106**, 2096.
Vanmunster, T. 2005, PERANSO period analysis software (version 2.1), www.peranso.com
Wilsey, N. J., and Beaky, M. M. 2009, in *The Society for Astronomical Sciences 28th Annual Symposium on Telescope Science*, held May 19–21, 2009, Big Bear Lake, CA, Soc. Astron. Sci., Rancho Cucamonga, CA, 107.
Wilson, R. E. 1994, *Publ. Astron. Soc. Pacific*, **106**, 921.
Wilson, R. E. 1979, *Astrophys. J.*, **234**, 1054.
Wilson, R. E., and Biermann, P. 1976, *Astron. Astrophys.,* **48**, 349.
Wilson, R. E., and Devinney, E. J. 1971, *Astrophys. J.*, **166**, 605.
Yilmaz, M., *et al.* 2009, *Inf. Bull. Var. Stars*, No. 5887.
Zejda, M. 2002, *Inf. Bull. Var. Stars*, No. 5287.
Zejda, M. 2004, *Inf. Bull. Var. Stars*, No. 5583.
Zhou, D.-Q., and Leung, K.-C. 1990, *Astrophys. J.*, **355**, 271.

Table 1. AC Bootis recalculated residuals $(O–C)_L$ following linear least squares fit of $(O–C)_1$ and cycle number between 16 Feb 2006 and 07 May 2009.

Time of Minimum	*Type Number*	*Cycle*	*$(O–C)_1$*	*$(O–C)_L$*	*Reference*
53782.5082	I	3639	–0.35389150	–0.001386	IBVS 5754
53798.5466	II	3684.5	–0.35189825	0.000614	IBVS 5754
53817.4000	I	3738	–0.35449300	–0.001973	IBVS 5761
53855.6428	II	3846.5	–0.35235525	0.000181	Present study
53859.5211	II	3857.5	–0.35098875	0.001549	IBVS 5713
53860.4008	I	3860	–0.35241000	0.000128	IBVS 5802
53862.5157	I	3866	–0.35220100	0.000338	IBVS 5707
53862.6921	II	3866.5	–0.35202525	0.000514	Present study
53884.7194	I	3929	–0.35275650	–0.000208	Present study
53895.4705	II	3959.5	–0.35133575	0.001217	IBVS 5731
53897.7599	I	3966	–0.35290100	–0.000347	Present study
53898.4647	I	3968	–0.35294800	–0.000394	IBVS 5731
53901.4619	II	3976.5	0.35156025	0.000995	IBVS 5731
53903.7514	I	3983	0.35301550	0.000459	Present study
53904.4553	I	3985	0.35397250	0.001416	IBVS 5761
53904.4562	I	3985	0.35307250	0.000516	IBVS 5754
53919.4375	II	4027.5	0.35083375	0.001729	IBVS 5761
53923.6644	II	4039.5	0.35331575	0.000751	Present study
53932.4785	II	4064.5	0.35042825	0.002140	IBVS 5761
53932.6518	I	4065	0.35334250	0.000774	Present study
53934.4142	I	4070	0.35319500	0.000626	IBVS 5761
53935.4711	I	4073	0.35364050	0.001071	IBVS 5761
54131.9628	II	4630.5	0.35197925	0.000672	IBVS 5820
54170.5550	I	4740	0.35289000	0.000222	IBVS 5802
54189.4124	II	4793.5	0.35148475	0.001191	IBVS 5801
54192.4074	I	4802	0.35229700	0.000380	IBVS 5898
54197.8699	II	4817.5	0.35274875	0.000070	IBVS 5814
54204.3908	I	4836	0.35214600	0.000536	IBVS 5889
54210.3819	I	4853	0.35267050	0.000014	IBVS 5802
54213.3783	II	4861.5	0.35208275	0.000603	IBVS 5874
54218.4880	I	4876	0.35288600	0.000198	IBVS 5802
54220.4258	II	4881.5	0.35355275	0.000864	IBVS 5802
54313.4732	II	5145.5	0.35255675	0.000171	IBVS 5830
54491.6398	I	5651	0.34867350	0.004129	IBVS 5887
54531.6382	II	5764.5	0.35317825	0.000359	IBVS 5898
54533.4012	II	5769.5	0.35242075	0.000399	IBVS 5898
54572.3454	I	5880	0.35378000	0.000944	IBVS 5897

Table 1 continued on following page

Table 1. AC Bootis recalculated residuals $(O–C)_L$ following linear least squares fit of $(O–C)_1$ and cycle number between 16 Feb 2006 and 07 May 2009, continued.

Time of Minimum	*Type*	*Number*	*Cycle*	*$(O–C)_1$*	*$(O–C)_L$*	*Reference*
54572.5224	II	5880.5	–0.35300425	–0.000168	IBVS 5697	
54595.4321	II	5945.5	–0.35245675	0.000389	IBVS 5889	
54597.5459	II	5951.5	–0.35334775	–0.000501	IBVS 5889	
54598.4267	I	5954	–0.35366900	–0.000822	IBVS 5889	
54600.5411	I	5960	–0.35396000	–0.001112	IBVS 5889	
54637.5482	I	6065	–0.35395250	–0.001089	IBVS 5889	
54639.4887	II	6070.5	–0.35191925	0.000945	IBVS 5889	
54643.3642	II	6081.5	–0.35335275	–0.000487	IBVS 5887	
54648.4743	I	6096	–0.35375600	–0.000888	IBVS 5889	
54671.3810	I	6161	–0.35620850	–0.003331	IBVS 5887	
54672.4404	I	6164	–0.35415400	–0.001276	IBVS 5889	
54942.4166	I	6930	–0.35350500	–0.000514	IBVS 5898	
54958.8099	II	6976.5	–0.34906025	0.003938	IBVS 5894	

Table 2. Comparison of selected geometrical and physical elements for AC Boo following Roche model light curve fitting.

Parameter[a]	*Mauder (1964) 1961*	*Binnendijk (1965) 1962*
T_1 (K)	6252	6252
T_2 (K)	6349 (6)	6349 (6)
q (m_2/m_1)	0.306 (0.002)	0.306 (0.002)
$A_{1,2}$	0.5	0.5
$g_{1,2}$	0.32	0.32
x_{1V}, y_{1V}	0.726, 0.269	0.726, 0.269
x_{2V}, y_{2V}	0.720, 0.272	0.720, 0.272
x_{1B}, y_{1B}	0.816, 0.212	0.816, 0.212
x_{2B}, y_{2B}	0.812, 0.221	0.812, 0.221
x_{1U}, y_{1U}	—	—
x_{2U}, y_{2U}	—	—
x_{1R}, y_{1R}	—	—
x_{2R}, y_{2R}	—	—
$\Omega_1 = \Omega_2$	2.4303 (0.005)	2.4303 (0.005)
i	84.03 (0.43)	84.03 (0.43)
r_1 pole	0.4645 (0.0013)	0.4645 (0.0007)
r_1 side	0.5020 (0.0018)	0.5020 (0.0010)
r_1 back	0.5308 (0.0020)	0.5308 (0.0011)
r_2 pole	0.2736 (0.0044)	0.2736 (0.0022)
r_2 side	0.2865 (0.0054)	0.2865 (0.0027)
r_2 back	0.3286 (0.0107)	0.3286 (0.0054)
$M_1/M_\odot$	1.688	1.688
$M_2/M_\odot$	0.517	0.517
$R_1/R_\odot$	1.367	1.367
$R_2/R_\odot$	0.813	0.813
$\Sigma (O–C)^2$	0.1111	0.0641
$A_{S1} = T_S/T$	0.75 (0.09)	—
Θ_{S1} (spot co-latitude)	90	—
ϕ_{S1} (spot longitude)	180	—
r_{S1} (angular radius)	10.0 (0.3)	—
$A_{S2} = T_S/T$	1.19 (0.04)	—
Θ_{S2} (spot co-latitude)	90	—
ϕ_{S2} (spot longitude)	210	—
r_{S2} (angular radius)	9.03 (0.38)	—

a: errors in parenthesis from WDWINT *v5.4e.*

Table 2 continued on following pages

Table 2. Comparison of selected geometrical and physical elements for AC Boo following Roche model light curve fitting, continued.

Parameter[a]	*Binnendijk (1965) 1963*	*Mancuso (1976) 1972*
T_1 (K)	6252	6252
T_2 (K)	6349 (6)	6349 (6)
q (m_2/m_1)	0.306 (0.002)	0.306 (0.002)
$A_{1,2}$	0.5	0.5
$g_{1,2}$	0.32	0.32
x_{1V}, y_{1V}	0.726, 0.269	0.726, 0.269
x_{2V}, y_{2V}	0.720, 0.272	0.720, 0.272
x_{1B}, y_{1B}	0.816, 0.212	—
x_{2B}, y_{2B}	0.812, 0.221	—
x_{1U}, y_{1U}	—	—
x_{2U}, y_{2U}	—	—
x_{1R}, y_{1R}	—	—
x_{2R}, y_{2R}	—	—
$\Omega_1 = \Omega_2$	2.4303 (0.005)	2.4303 (0.005)
i	84.03 (0.43)	84.03 (0.43)
r_1 pole	0.4645 (0.0006)	0.4645 (0.0013)
r_1 side	0.5020 (0.0008)	0.5020 (0.0018)
r_1 back	0.5308 (0.0009)	0.5308 (0.0019)
r_2 pole	0.2736 (0.0019)	0.2736 (0.0050)
r_2 side	0.2865 (0.0024)	0.2865 (0.0062)
r_2 back	0.3286 (0.0046)	0.3286 (0.0122)
$M_1/M_\odot$	1.688	1.688
$M_2/M_\odot$	0.517	0.517
$R_1/R_\odot$	1.367	1.367
$R_2/R_\odot$	0.813	0.813
$\Sigma (O–C)^2$	0.0787	0.1613
$A_{S1} = T_S/T$	0.75 (0.02)	0.85 (0.03)
Θ_{S1} (spot co-latitude)	90	90
ϕ_{S1} (spot longitude)	180	180
r_{S1} (angular radius)	10.7 (0.1)	8.06 (0.43)
$A_{S2} = T_S/T$	11.22 (0.01)	—
Θ_{S2} (spot co-latitude)	90	—
ϕ_{S2} (spot longitude)	200	—
r_{S2} (angular radius)	913.75 (0.18)	—

a: errors in parenthesis from wdwint v5.4e.

Table 2 continued on following pages

Table 2. Comparison of selected geometrical and physical elements for AC Boo following Roche model light curve fitting, continued.

Parameter[a]	*Mancuso (1976) 1973*	*Schieven (1983) 1982*
T_1 (K)	6252	6252
T_2 (K)	6349 (6)	6349 (6)
q (m_2/m_1)	0.306 (0.002)	0.306 (0.002)
$A_{1,2}$	0.5	0.5
$g_{1,2}$	0.32	0.32
x_{1V}, y_{1V}	0.726, 0.269	0.726, 0.269
x_{2V}, y_{2V}	0.720, 0.272	0.720, 0.272
x_{1B}, y_{1B}	—	0.816, 0.212
x_{2B}, y_{2B}	—	0.812, 0.221
x_{1U}, y_{1U}	—	0.858, 0.188
x_{2U}, y_{2U}	—	0.852, 0.213
x_{1R}, y_{1R}	—	—
x_{2R}, y_{2R}	—	—
$\Omega_1 = \Omega_2$	2.4303 (0.005)	2.4303 (0.005)
i	84.03 (0.43)	84.03 (0.43)
r_1 pole	0.4645 (0.0013)	0.4645 (0.0008)
r_1 side	0.5020 (0.0017)	0.5020 (0.0011)
r_1 back	0.5308 (0.0010)	0.5308 (0.0013)
r_2 pole	0.2736 (0.0048)	0.2736 (0.0026)
r_2 side	0.2865 (0.0059)	0.2865 (0.0032)
r_2 back	0.3286 (0.0117)	0.3286 (0.0063)
$M_1/M_\odot$	1.688	1.688
$M_2/M_\odot$	0.517	0.517
$R_1/R_\odot$	1.367	1.367
$R_2/R_\odot$	0.813	0.813
$\Sigma (O–C)^2$	0.0843	0.0435
$A_{S1} = T_S/T$	0.78 (0.03)	—
Θ_{S1} (spot co-latitude)	90	—
ϕ_{S1} (spot longitude)	180	—
r_{S1} (angular radius)	10.5 (0.4)	—
$A_{S2} = T_S/T$	—	1.15 (0.01)
Θ_{S2} (spot co-latitude)	—	90
ϕ_{S2} (spot longitude)	—	140
r_{S2} (angular radius)	—	10.60 (0.22)

a: errors in parenthesis from wdwint v5.4e.

Table 2 continued on following page

Table 2. Comparison of selected geometrical and physical elements for AC Boo following Roche model light curve fitting, continued.

Parameter[a]	*Robb (1985) 1984*	*Present 2006*
T_1 (K)	6252	6252
T_2 (K)	6349 (6)	6349 (6)
q (m_2/m_1)	0.306 (0.002)	0.306 (0.002)
$A_{1,2}$	0.5	0.5
$g_{1,2}$	0.32	0.32
x_{1V}, y_{1V}	0.726, 0.269	0.726, 0.269
x_{2V}, y_{2V}	0.720, 0.272	0.720, 0.272
x_{1B}, y_{1B}	0.816, 0.212	—
x_{2B}, y_{2B}	0.812, 0.221	—
x_{1U}, y_{1U}	0.858, 0.188	—
x_{2U}, y_{2U}	0.852, 0.213	—
x_{1R}, y_{1R}	—	0.634, 0.276
x_{2R}, y_{2R}	—	0.627, 0.279
$\Omega_1 = \Omega_2$	2.4303 (0.005)	2.4303 (0.005)
i	84.03 (0.43)	84.03 (0.43)
r_1 pole	0.4645 (0.0018)	0.4645 (0.0006)
r_1 side	0.5020 (0.0024)	0.5020 (0.0007)
r_1 back	0.5308 (0.0027)	0.5308 (0.0008)
r_2 pole	0.2736 (0.0056)	0.2736 (0.0018)
r_2 side	0.2865 (0.0068)	0.2865 (0.0022)
r_2 back	0.3286 (0.0134)	0.3286 (0.0043)
$M_1/M_\odot$	1.688	1.688
$M_2/M_\odot$	0.517	0.517
$R_1/R_\odot$	1.367	1.367
$R_2/R_\odot$	0.813	0.813
$\Sigma (O–C)^2$	0.0782	0.0157
$A_{S1} = T_S/T$	—	1.20 (0.01)
Θ_{S1} (spot co-latitude)	—	35
ϕ_{S1} (spot longitude)	—	10
r_{S1} (angular radius)	—	14.8 (0.2)
$A_{S2} = T_S/T$	0.96 (0.01)	1.20 (0.01)
Θ_{S2} (spot co-latitude)	90	90
ϕ_{S2} (spot longitude)	180	340
r_{S2} (angular radius)	15.3 (1.1)	18.5 (0.5)

a: errors in parenthesis from wdwint v5.4e.

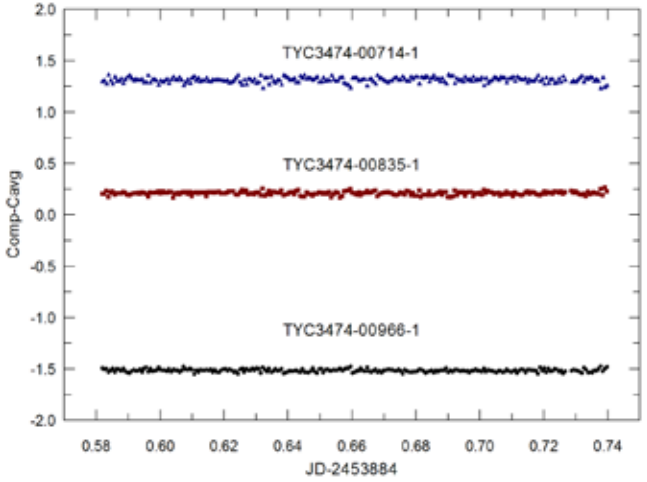

Figure 1. Constant relative magnitude (*V*-band) exhibited by comparison stars during a typical AC Boo photometric session (29 May 2006).

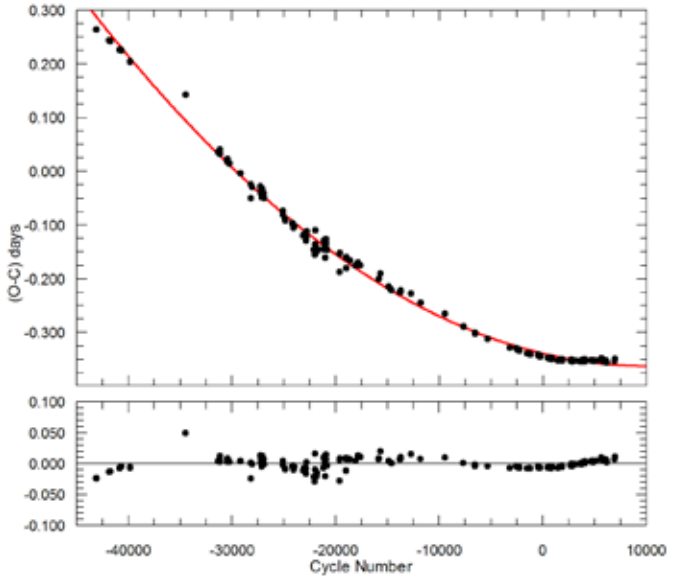

Figure 2. Quadratic least square fit of residuals $(O–C)_1$ as a function of cycle number for AC Boo observed between 18 Jan 1961 and 07 May 2009 (top panel). Quadratic residuals $(O–C)_Q$ are shown in the bottom panel.

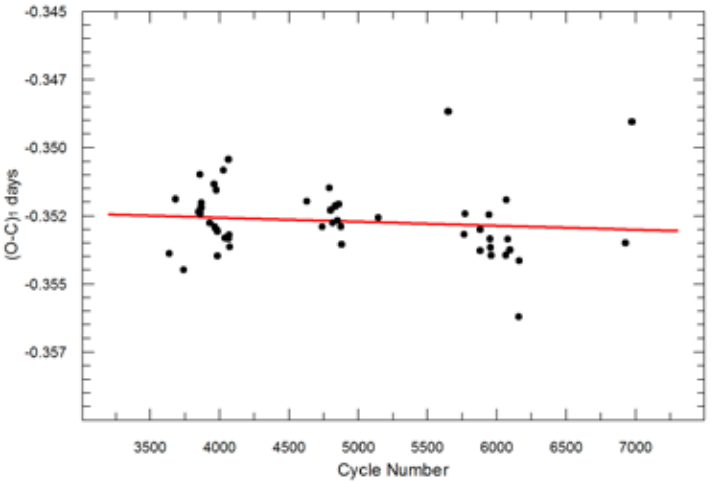

Figure 3. Near term simple least squares fit of residuals $(O–C)_1$ as a function of cycle number for AC Boo observed between 16 Feb 2006 and 07 May 2009.

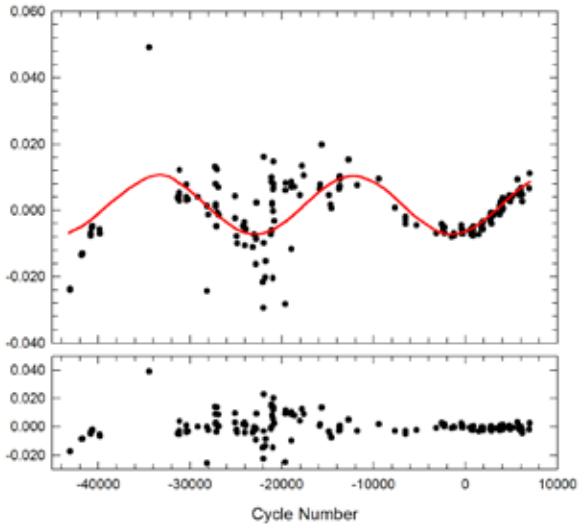

Figure 4. Fourier transform of quadratic residuals $(O–C)_Q$ calculated for AC Boo between 18 Jan 1961 and 07 May 2009 (top panel). The sinusoidal-like periodicity (P~21 years) is strongly influenced by the fit of data over the past two decades (cycle –14000 to 6977). Corresponding residuals (O–C)S are plotted in the bottom panel.

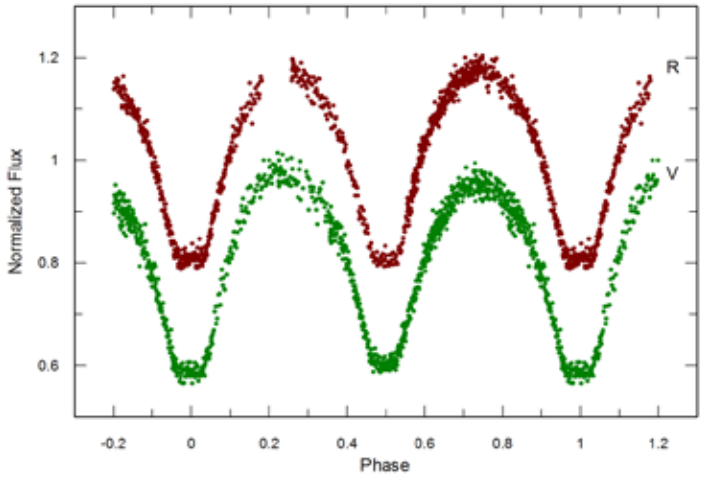

Figure 5. Folded CCD-derived light curves for AC Boo captured in *V*- (April–July 2006) and *R*-band (June–July 2006). Curves in each passband are offset for clarity.

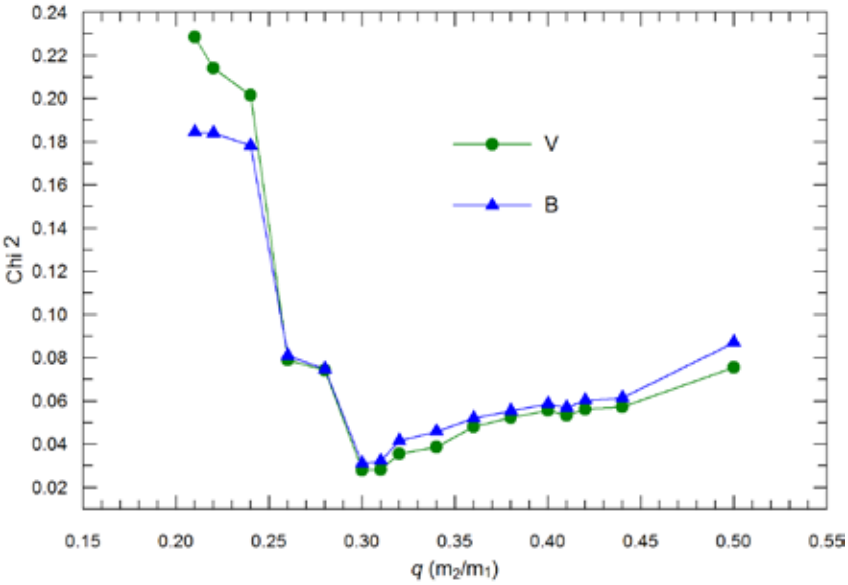

Figure 6. Photometric search for AC Boo mass ratio (m_2/m_1) using Roche modeling of 1962 light curves from Binnendijk (1965).

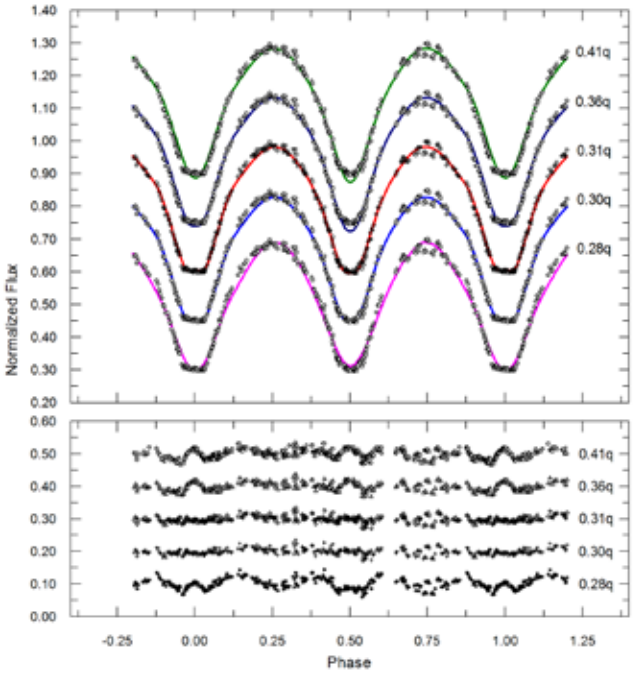

Figure 7. Series of Roche model predictions using varying values for q with the 1962 light curve (V-band) reported by Binnendijk (1965).

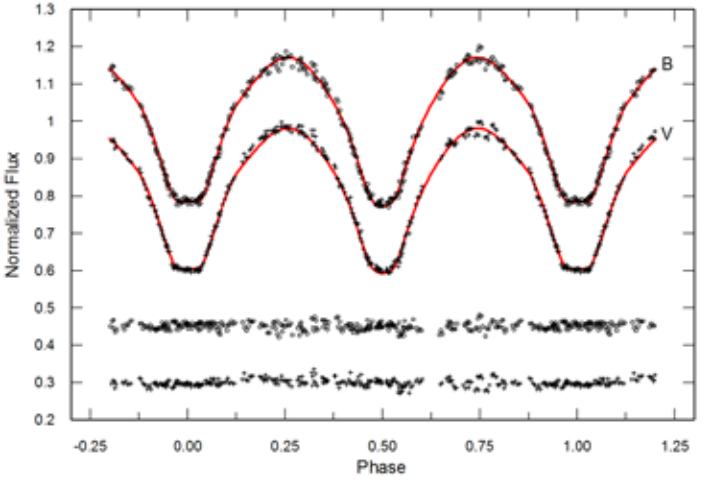

Figure 8. V- and B-band light curves for AC Boo captured in 1962 by Binnendijk (1965). Solid line represents the best theoretical fit using the Roche model without invoking spots. Light curves (top) and model fit residuals (bottom) in each passband are offset for clarity.

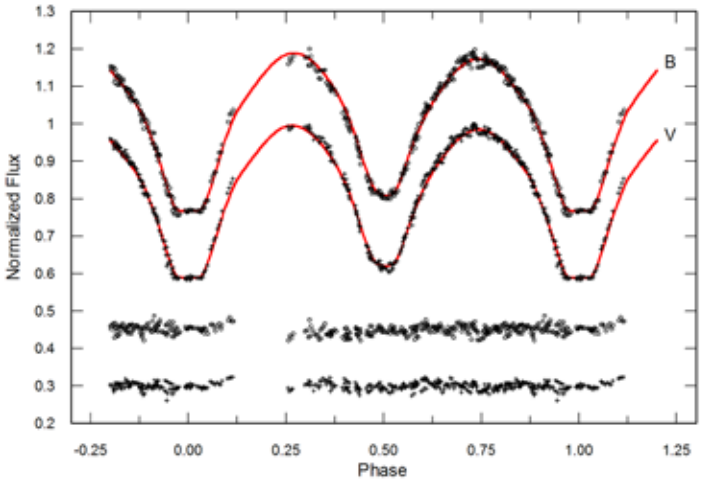

Figure 9. *V*- and *B*-band photoelectric light curves for AC Boo captured in 1963 by Binnendijk (1965). Solid line is the best theoretical fit using the Roche model with a single hot (secondary) and cool (primary) spot on each star. Light curves (top) and model fit residuals (bottom) are offset for clarity.

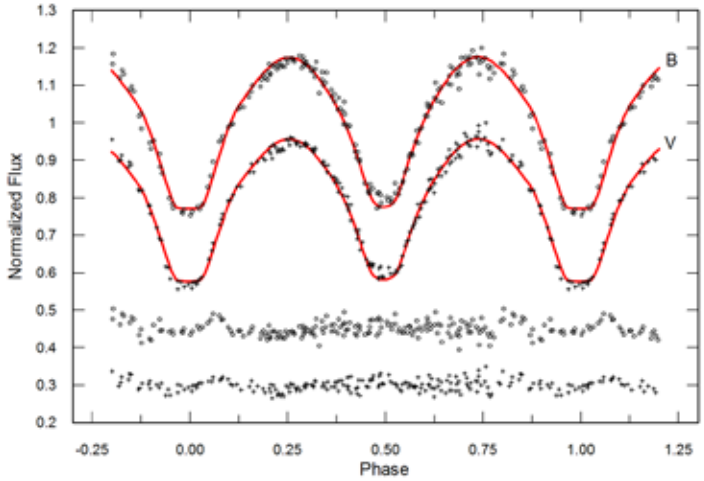

Figure 10. *V*- and *B*-band photoelectric light curves for AC Boo captured in 1961 by Mauder (1964). Solid line represents the best theoretical fit using the Roche model with a single hot (secondary) and cool (primary) spot on each star. Light curves (top) and model fit residuals (bottom) are offset for clarity.

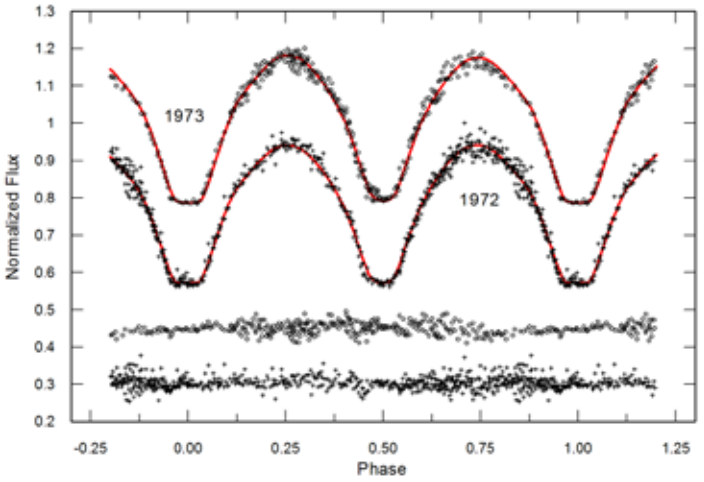

Figure 11. *V*-band photoelectric light curves for AC Boo acquired in 1972 (bottom) and 1973 (top) by Mancuso *et al.* (1976). Solid line is the best theoretical fit using the Roche model with a single cool spot on the primary. Light curves (top) and model fit residuals (bottom) for each year are offset for clarity.

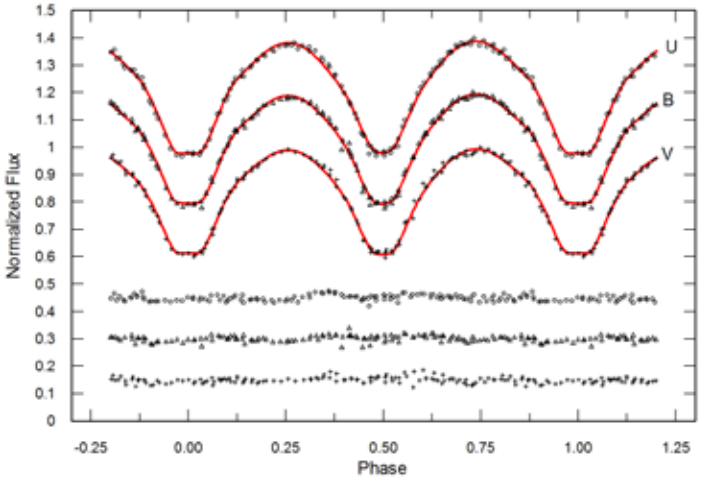

Figure 12. *U*-, *B*- and *V*-band photoelectric light curves for AC Boo captured in 1982 by Schieven *et al.* (1983). Solid line represents the best theoretical fit using the Roche model with a hot spot on the less massive star. Light curves (top) and model fit residuals (bottom) in each passband are offset for clarity.

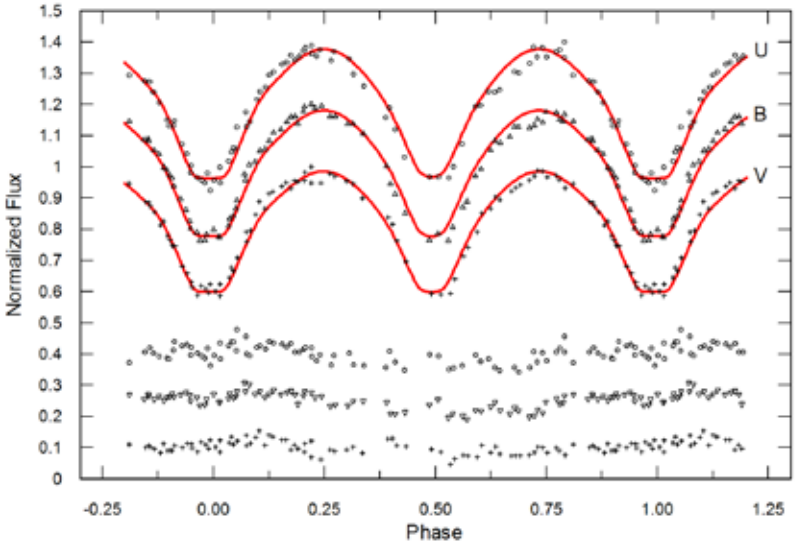

Figure 13. *U*-, *B*- and *V*-band photoelectric light curves for AC Boo acquired in 1984 by Robb (1985). Solid line represents the best theoretical fit using the Roche model with a cool spot on the more massive star. Light curves (top) and model fit residuals (bottom) in each passband are offset for clarity.

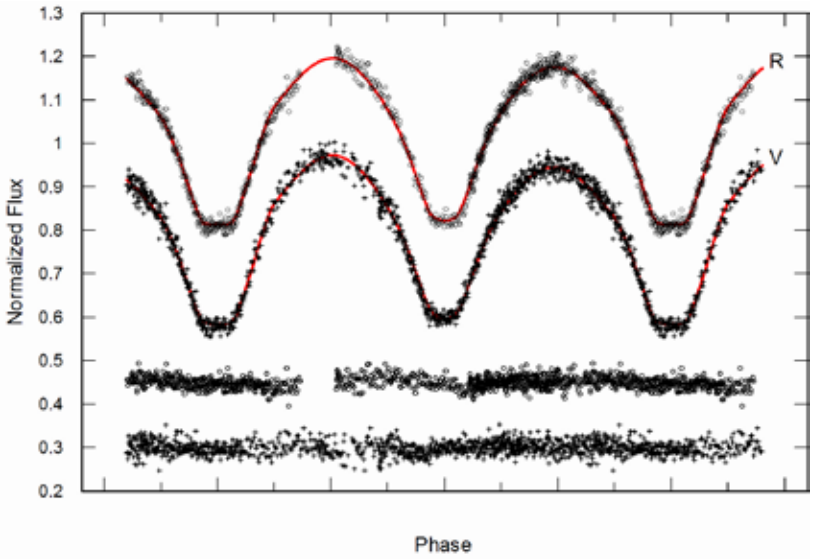

Figure 14. *R*- and *V*-band CCD light curves for AC Boo captured in 2006 (present study). Solid line represents the best theoretical fit using the Roche model with a hot spot on each star. Light curves (top) and model fit residuals (bottom) for each passband are offset for clarity.

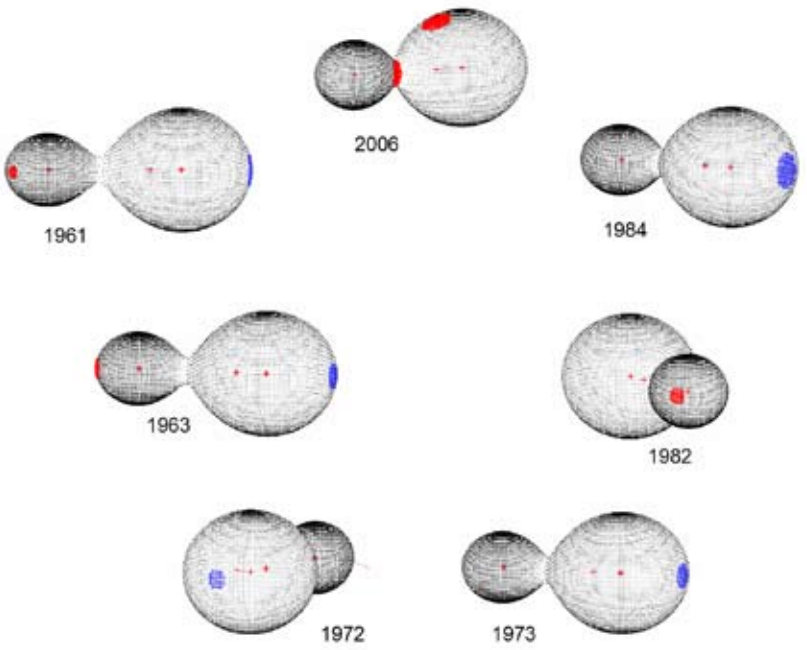

Figure 15. Three-dimensional renderings of Roche lobe geometry for the W-type W UMa overcontact binary AC Boo showing starspot locations from 1961 to 2006. Images were produced using BINARYMAKER 3.